Crossover from superspin glass to superferromagnet in Fe$_x$Ag$_{100-x}$ nanostructured thin films ($20 \le x \le 50$)

J. Alonso, M. L. Fdez-Gubieda, J. M. Barandiarán, and A. Svalov
Departamento de Electricidad y Electrónica, Universidad del País Vasco (UPV/EHU), Apartado 644, 48080 Bilbao, Spain

L. Fernández Barquín and D. Alba Venero
CITIMAC, Universidad de Cantabria, 39005 Santander, Spain

I. Orue
SGiker, Universidad del País Vasco (UPV/EHU), Apartado 644, 48080 Bilbao, Spain

Fe$_x$Ag$_{100-x}$ granular thin films, with $20 \le x \le 50$, have been prepared by the dc-magnetron sputtering deposition technique. With this technique we have been able to obtain samples comprising small Fe nanoparticles (2.5–3 nm) embedded in a Ag matrix, remaining their size practically constant with increasing Fe content. Their magnetic behavior has been fully characterized by dc magnetic measurements between 5–350 K. They have revealed a crossover in the collective magnetic behavior of the Fe nanoparticles around a 35 at. %. Below such a concentration, a collective freezing of the magnetic moments is observed at low temperatures, while at high temperatures a transition, mainly mediated by dipolar interactions, to a magnetically disordered state is obtained. Above this concentration, direct exchange interactions overcome the dipolar magnetic interactions and a long-range order tends to prevail in the range of temperatures analyzed. ac magnetic measurements have indicated a crossover from a superspin glass ($x < 35$) to a superferromagnetic ($x > 35$) behavior for the magnetic moments of the Fe nanoparticles.

PACS number(s): 75.30.Kz, 75.70.Ak, 75.40.Gb

I. INTRODUCTION

The study of the magnetic behavior of ensembles of magnetic nanoparticles has attracted great attention from material scientists for several years.[1–5] The appeal of these systems arises from the complexity and variety of the magnetic interactions among the magnetic nanoparticles, as well as the technological potential based on, for instance, giant magnetoresistance or ultrasoft magnetic properties.[6,7] At very low concentrations, each of the nanoparticles behaves individually like a superparamagnet.[8] As the concentration increases, interparticle magnetic interactions become more relevant and a collective magnetic behavior is found. The understanding of these collective behaviors is important not only from a theoretical point of view, but also for technological applications, as magnetic memories or sensitive magnetic field sensors.[9]

Binary Fe$_x$Ag$_{100-x}$ granular thin films are ideal systems to study these phenomena since Fe and Ag present a high value of positive alloy formation energy (28 kJ/mol),[10] thereby being highly immiscible and allowing us to obtain samples consisting of an assembly of Fe nanoparticles embedded in a diamagnetic metallic Ag matrix for a wide range of compositions. Their magnetic and magnetotransport properties have been previously studied.[1,2,11,12] As observed by Binns *et al.*[1] for sputtered Fe-Ag granular thin films, at very low atomic concentrations ($\le 2\%$) these thin films fulfill the conditions for ideal superparamagnetism (SPM): the magnetic behavior is given by the average over a set of independent noninteracting nanoparticles. Single-particle blocking is thus observed at very low temperatures (~ 5 K). At atomic fractions up to $\le 25\%$, the high-temperature behavior can be described

as interacting superparamagnetism (ISPM) (see Allia *et al.*[13]): the sample consists of aggregates of nanoparticles which interact by dipolar magnetic interactions, mainly, and as the temperature decreases, a collective freezing of the moments of the aggregates is observed. At high compositions ($\ge 60\%$) and above ~ 50 K, the magnetic configuration is typical of a correlated supersping glass (CSSG), in which random deviation of the moments from alignment produces a smooth rotation of the magnetization throughout the system with a correlation length much larger than the diameter of the nanoparticles. However, while the range of Fe concentrations corresponding to low ($x < 25$) and high ($x \gg 50$) Fe content has been widely analyzed, there are still many questions concerning the intermediate range (25–50 %) and the nature of the different competing factors which play a significant role at these particular concentrations.

However, for Co$_{80}$Fe$_{20}$ nanoparticles embedded in *glassy* Al$_2$O$_3$ with nanoparticle concentrations below their physical three-dimensional percolation, Kleemann *et al.*[14] have proposed mainly two kinds of collective magnetic states. For an intermediate strength of dipolar interactions and randomness of particle positions, one can observe a supersping glass state (SSG).[15] Here the supersping (magnetic nanoparticles) freeze collectively into a spin glass-like state at low temperatures and low concentrations. For higher densities of nanoparticles, and hence stronger interactions, one can observe a superferromagnetic state (SFM), characterized by ferromagnetic interparticle correlations.[16] The terms supersping glass and superferromagnetism were first coined by Mørup *et al.*[17] to explain the magnetic behavior of interacting crystallites of antiferromagnetic goethite.

With increasing particle density, the role of magnetic interactions among nanoparticles becomes non-negligible and

one finds a crossover from single-particle blocking to collective freezing. Therefore, we are going to study the range of concentrations around which this collective freezing takes place. In this paper we face an in-depth study of the magnetic behavior of small Fe nanoparticles inside sputter deposited Fe_xAg_{100-x} granular thin films with Fe concentrations $20 \leq x \leq 50$. For these granular systems, we have carried out an intensive characterization of their magnetic behavior and analyzed the evolution of the collective magnetic states with increasing Fe content. These are modulated mainly by the competition between interparticle magnetic interactions, the intraparticle anisotropy, the externally applied magnetic field and the thermal disorder. In order to gain a better description of these collective magnetic states, apart from the typical dc magnetic measurements, we have also performed a frequency-dependent ac susceptibility analysis.

II. EXPERIMENTAL DETAILS

Fe_xAg_{100-x} granular thin films were prepared by sputtering deposition, with composition $20 \leq x \leq 50$, as determined by energy dispersive x-ray analysis. These concentrations are slightly higher than those indicated by the magnetic saturation values and fall within the experimental error. The Fe-Ag samples were deposited by dc magnetron sputtering at room temperature onto Si(100) substrates, using a Pfeiffer Vacuum Classic 500 system, being the base pressure $\sim 10^{-7}$ mbar with approximately 2×10^{-3} mbar of Ar. The target consisted of a certain number of Fe chips placed on an Ag disk. By varying the number of Fe chips we managed to obtain different Fe concentrations from 20 to 50 at. % Fe. The thickness of the Fe-Ag thin films were kept between 100–150 nm (± 10 nm) as measured by atomic force microscopy and the final samples were covered with ~ 10 nm of Au in order to avoid oxidation. During the deposition, we used an Al sputtering mask covering the substrate to obtain films of the same shape (squares of 3×3 mm^2), which is very important in order to properly compare the results obtained for the different Fe-Ag samples. Magnetic measurements were performed in a superconducting quantum interference device magnetometer (Quantum Design MPMS-7). Zero-field-cooling/field-cooling (ZFC/FC) measurements $[M(T)]$ were carried out in both dc and ac mode. dc magnetization curves were measured with different applied magnetic fields (μ_0H =0.5, 1.5, 2.5, 5, and 10 mT) in the temperature range $0 < T < 350$ K. ac susceptibility measurements were carried out in the same range of temperatures but with an applied field $\mu_0h=0.3$ mT and at several frequencies ($0.03 < f < 1000$ Hz). All the magnetic measurements have been normalized to the volume of the Fe-Ag thin film (3 mm $\times 3$ mm $\times$ thickness), which allow us to give absolute values in magnetization with an error of $\sim 8\%$

III. RESULTS AND DISCUSSION

A. dc magnetometry

First of all, we have evaluated the thermal dependence of the magnetization by the usual procedure of ZFC/FC. In our case, we have carried out ZFC/FC measurements from 5 to
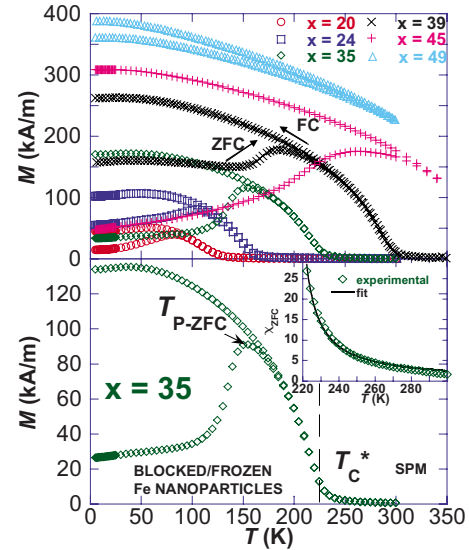

FIG. 1. (Color online) (Top) ZFC/FC curves for Fe_xAg_{100-x} ($20 \leq x \leq 49$) (bottom) ZFC/FC curves for samples $Fe_{35}Ag_{65}$. In the inset, the fitting to a Curie-Weiss law is depicted.

350 K applying an external dc magnetic field of 0.5 mT. This field has been initially kept small enough not to mask the subtle magnetic phenomena taking place during the ZFC/FC process.

Figure 1 (top) shows these ZFC/FC curves for Fe_xAg_{100-x} being $x=20$, 24, 35, 39, 45, and 49. As can be seen, during the FC process the magnetization decreases progressively with increasing temperature, except for a small peak centered at low temperatures, T_{P-FC}, and overlaps the ZFC curve above a certain irreversibility temperature T_{irr}. The irreversibility is a proof of the magnetic disorder produced by the interparticle interactions (exchange and dipolar, mainly), the nanoparticle anisotropy and the random position of the nanoparticles. On the other hand, during the ZFC process the magnetization generally increases with increasing temperature until reaching a certain maximum at T_{P-ZFC} [as exemplified in Fig. 1 (bottom)]. However, for some samples there is some remanent contribution to the magnetization at low temperatures. This is due to the deposition process and relates to the magnetic fields inside the magnetron sputtering chamber. In order to minimize its effects, we have carried out a demagnetization process for each of the analyzed samples just before measuring them. Above T_{P-ZFC}, the magnetization starts to decay in a Curie-Weiss way, becoming completely null at high enough temperatures. This can be explicitly seen in the inset of Fig. 1 (bottom), where the good fitting of the experimental ZFC curve to the Curie-Weiss expression $[\chi = C/(T - T_C^*)]$ is depicted. T_C^* corresponds to the Curie temperature and its value depends on the nature of the interactions. C is the Curie constant which depends on the average volume V of the nanoparticles: $C = x'VM_S^2\mu_0/3k_B$, being M_S the saturation magnetization of Fe (1745 kA/m at 0 K), x' the volume concentration of the nanoparticles ($0 < x' < 1$), and $V = (\pi/6)D^3$, where D is the average diameter of the magnetic nanoparticles. The values of T_C^* and D obtained from these fittings are indicated in Table I, together with the corresponding values of T_{P-ZFC} and T_{irr}. As can be seen, T_C^* is

TABLE I. $T_{P\text{-}ZFC}$, $T_{P\text{-}FC}$, T_{irr}, T_C^*, and D values obtained for Fe_xAg_{100-x} ($x=20$, 24, 35, 39, 45, and 49).

	$T_{P\text{-}ZFC}$ (K)	$T_{P\text{-}FC}$ (K)	T_{irr} (K)	T_C^* (K)	D (nm)
$x=20$	86.5 ± 0.5	58.5 ± 0.5	105.3 ± 0.5	119.4 ± 0.2	2.7 ± 0.4
$x=24$	103.2 ± 0.5	48.1 ± 0.5	133.2 ± 0.5	151.7 ± 0.2	2.9 ± 0.6
$x=35$	155.0 ± 0.5	37.5 ± 0.5	194.9 ± 0.5	221.9 ± 0.2	2.6 ± 0.5
$x=39$	184.5 ± 0.5	26.7 ± 0.5	297.8 ± 0.5	286.8 ± 0.1	2.5 ± 0.4
$x=45$	262.5 ± 0.5	14.5 ± 0.5			
$x=49$		12.0 ± 0.5			

always positive, indicating the major ferromagnetic nature of the interactions. D is around 2.5–3 nm for the samples with $20 \leq x \leq 40$. From the fitting of the hysteresis cycles $[M(H)$ curves measured at room temperature for $x=20]$ to an ISPM model (not shown here), we have also obtained an average diameter for our isolated nanoparticles of 2.5 nm. Remarkably, D remains quite constant with increasing Fe content. At high Fe content ($>40\%$), the magnetic transition shifts to higher temperatures and gets out of the range of temperatures analyzed, so we can no longer carry out the fitting. Since the size of the nanoparticles keeps quasiconstant, our thin films present as an ideal system in order to study the evolution of the collective magnetic behavior of the system as the magnetic density increases with increasing Fe content.

The shape of the ZFC/FC curves changes progressively with increasing Fe concentration. The maximum in the ZFC curve becomes wider and shifts to higher temperatures. Normally, a broadening phenomenon of the ZFC peak is related to an increase in the size distribution of the nanoparticles or to an effect of the interactions.[18] Taking into account the previous results for the evolution of the average size with the Fe content and that we are working at considerably high Fe concentrations, it is clear that this broadening must be mostly related to the increasing importance of interactions in general and short-range ferromagnetic interactions in particular, as the density of nanoparticles increases and the interparticle distances are shortened. For the sample with the highest Fe concentration ($x=49$) no maximum has been measured in the ZFC curve and the thermal evolution is very similar to that of the FC curve. $T_{P\text{-}ZFC}$, T_C, and T_{irr} also displace to higher temperatures as the Fe amount increases, as indicated in Table I. If we plot these temperatures against the Fe concentration in our samples we obtain an interesting divergence. As depicted in Fig. 2, the values of all these temperatures follow the same linear evolution up to a 35 at. % Fe. After that concentration, the slope of this linear evolution suffers an appreciable increase (approximately twofold) for all the previous temperatures at the same time. This clearly reveals a change in the collective magnetic behavior of the Fe-Ag thin films as a function of the Fe concentration.

Another remarkable point is the appearance of a small peak at low temperatures ($T_{P\text{-}FC}$) in the FC curve, as shown in Fig. 3. In superparamagnets, the FC magnetization always increases as the temperature is decreased. This is simply because superspins are blocked in the direction of the field. A peak in the FC curve like the one obtained for our samples has been experimentally observed in superspin glass sys-

tems, such as Fe_3N nanoparticle systems,[19] and can be related to the presence of strong magnetic dipolar interactions as has been shown by Monte Carlo simulations, using a model which includes a summation of dipole fields to take account of the interactions.[20,21] Since this peak disappears with increasing Fe content, it indicates that the ferromagnetic exchange interactions progressively overcome the spin glass-like disorder at low temperatures.

We have further studied the thermal evolution of the magnetization in our samples by analyzing the evolution of the ZFC/FC curves as a function of the applied magnetic field H. We have focused on the differences in the magnetic response for samples with concentrations above and below $x=35$, which marks the crossover. In Fig. 4 we present the ZFC/FC curves for the samples $Fe_{20}Ag_{80}$ and $Fe_{45}Ag_{55}$ measured at $\mu_0H=0.5$, 1.5, 2.5, 5, and 10 mT. As can be seen, the evolution of the ZFC/FC curves with the applied field is completely different depending on the composition. For the sample with $x<35$ (Fig. 4 top), as we raise the magnetic field, the ZFC/FC curves become slightly wider and displace toward lower temperatures. We obtain an slow decrease of $T_{P\text{-}ZFC}$ and $T_{P\text{-}FC}$, and an slight increase of T_C^* with increasing H. This behavior is typical of systems with preponderant dipolar magnetic interactions, due to the anisotropic nature of the dipolar interactions, even if there is a certain degree of ferromagnetic behavior. The response to the field is thereby relatively weak as precisely observed in the evolution of the ZFC/FC curves for this $Fe_{20}Ag_{80}$ thin film. Moreover, we have observed that as the applied magnetic field increases, the FC peak becomes less appreciable and displaces toward lower temperatures as it is typical, again, of samples with dipolar magnetic interactions.[20] On the other hand, for samples with $x>35$ (Fig. 4 bottom), the magnetic response
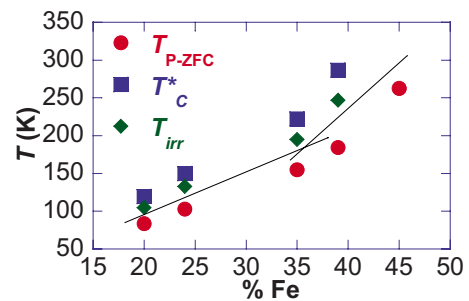

FIG. 2. (Color online) Evolution of the characteristic temperatures $T_{P\text{-}ZFC}$, T_{irr}, and T_C^* as a function of the Fe content. Lines are guide for the eyes and the error bars are smaller than the symbols.
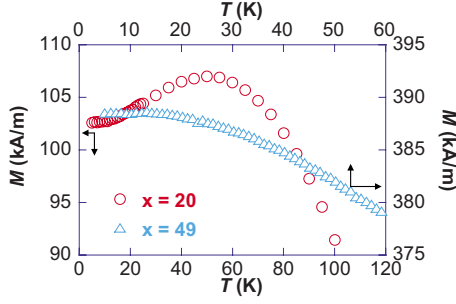
FIG. 3. (Color online) Detail of the FC peak at low temperatures for Fe_xAg_{100-x} ($x=20$ and 49).

is notably faster. Both $T_{P\text{-}ZFC}$, $T_{P\text{-}FC}$, and T_{irr} displace toward much lower temperatures, smearing out the irreversibility for an applied field of $\mu_0H=5$ mT. These differences in the thermal magnetic response depending on the Fe concentration of our samples are more clearly appreciated in Fig. 5, where the evolution of the $T_{P\text{-}ZFC}$ vs H is represented. As shown, by increasing the field from 0.5 to 2.5 mT, $T_{P\text{-}ZFC}$ reduces in a $\sim30\%$ and 80% for the samples with $x=20$ and 45, respectively. This can be easily explained because at high Fe concentrations, the Fe nanoparticles are correlated via direct exchange interactions, allowing them to align their magnetic moments in the direction of the applied magnetic field much more faster than at low Fe content.

We have tried to fit the experimental curves of Fig. 5 to an appropriate phenomenological model in order to obtain some information about the evolution of the correlation lengths and the anisotropies as a function of the concentration. In order to take into account the interaction effects on the field dependence of $T_{P\text{-}ZFC}$, we have employed an expression based on a modified version of the random anisotropy model[22] that can be used to describe the magnetic behavior of granular systems. This model takes into account the concentration and size of the nanoparticles, as well as the field dependence of the correlation length, and allows a quantita-
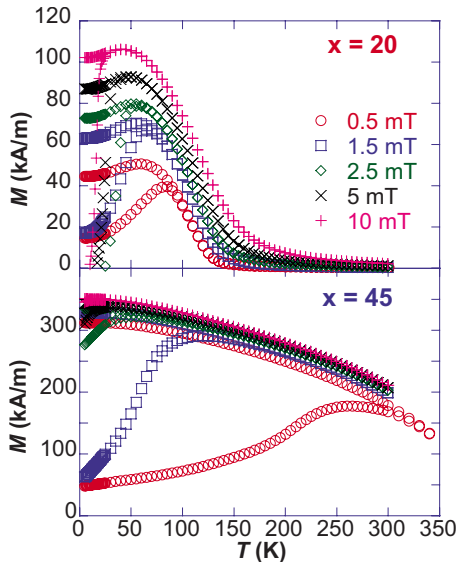

FIG. 4. (Color online) ZFC/FC curves for $Fe_{20}Ag_{80}$ (top) and $Fe_{45}Ag_{55}$ (bottom) measured at $\mu_0H=0.5$, 1.5, 2.5, 5, and 10 mT.
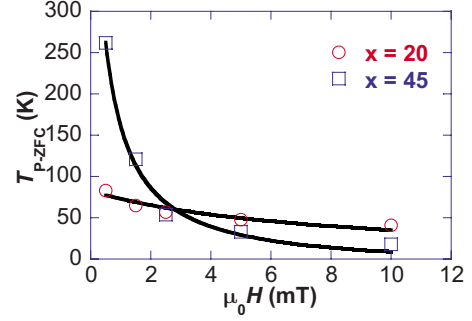

FIG. 5. (Color online) Evolution of $T_{P\text{-}ZFC}$ for $Fe_{20}Ag_{80}$ and $Fe_{45}Ag_{55}$ as a function of the applied field $\mu_0H=0.5$, 1.5, 2.5, 5, and 10 mT, and their corresponding fitting to a phenomenological expression based on a modified random anisotropy model.

tive analysis of the field dependence of the blocking temperature [$T_{P\text{-}ZFC}(H)$], which is given by the following expression:

$$T_{P\text{-}ZFC}(H) = \frac{K\pi[D^3 + x'(L_H^3 - D^3)]}{6k_B \ln(\tau_m/\tau_0)\{1 + x[(L_H^3 - D^3)]/D^3\}^{1/2}} \times \left\{1 - \frac{HM_S[1 + x'(L_H^3 - D^3)/D^3]^{1/2}}{2K}\right\}^{1.5}$$

(1)

being $L_H = D + [2A/(M_SH+C)]^{1/2}$ the correlation length as a function of the applied field, that gives a measure of the average distance over which magnetization fluctuations are correlated. A represents the interaction intensity, which for nanogranular systems corresponds to the intergranular exchange constant. K represents the anisotropy of the nanoparticles, D is their diameter, x' is the volume concentration of the nanoparticles ($0 < x' < 1$), τ_0 corresponds to the characteristic relaxation time of the magnetic moments ($10^{-9} - 10^{-10}$ s), τ_m is the measurement time (typically in the order of 100 s for dc measurements), and M_S is the saturation magnetization of Fe. The parameter C is included in order to overcome the divergence of L_H at zero field. It is expected that C approaches zero for systems of clustered nanoparticles, and increases with the progressive dilution. We have used this expression to fit our experimental data, as shown in Fig. 5. The fits represented by the solid lines were carried out by using the following data: $D=2.5$ nm, $\tau_0=10^{-9}$ s, and $\tau_m=100$ s. We have also fixed the value of $A=3.3 \times 10^{-12}$ J/m, a value obtained by Binns *et al.*[1] for thin films composed of pure Fe clusters and applied with good results in Monte Carlo simulations for a wide range of Fe concentrations in the case of Fe-Ag granular thin films. K and L_H have been left as free parameters. A good fitting is obtained with this model, as shown in Fig. 5. The values obtained for K and the correlation length at zero applied field L_0 are represented in Table II. As can be seen, K becomes smaller with increasing x while L_0 rapidly increases. The obtained K values are significantly larger than those corresponding to bulk Fe, as it is usual in nanogranular systems, and compare very well with those estimated for Fe-Ag granular thin films (1.75×10^5 J/m^3 for $x=25$) (Ref. 1) or with those reported

TABLE II. K and L_0 parameters obtained from the fittings of the T_B vs H to an expression based on a modified random anisotropy model for Fe_xAg_{100-x} ($x=20$ and 45).

	K (J/m^3)	L_0 (nm)
$x=20$	$3.0 \pm 0.8 \times 10^5$	24 ± 6
$x=45$	$1.8 \pm 0.1 \times 10^5$	92 ± 4

in FeCuAg granular alloys (4.41×10^5 J/m^3) (Ref. [23]) and in CoCu granular alloys (2×10^5 J/m^3).[24] For the samples with low concentrations, the relaxations in each particle remains governed mainly by their anisotropic barriers. As the concentration increases, the anisotropy decreases since the percolation among the nanoparticles diminishes the effect of the effective anisotropy. On the other hand, $L_0 > D$ even for the sample with $x=20$. For this sample, magnetically correlated clusters of several particles are formed which interact mainly by dipolar interactions (the coercive field obtained from the $M(H)$ curves is quite large $\mu_0 H_C = 32.3$ mT, at 5 K). However for the sample with $x=45$, $L_0 \gg D$, indicating an important clusterization of the nanoparticles (the coercivity decreases, $\mu_0 H_C = 11.4$ mT, at 5 K). Therefore, as the Fe concentration increases it becomes more difficult to identify the individual nanoparticles and largely correlated clusters are progressively formed, changing the overall magnetic behavior of our samples.

To sum up, from this dc analysis we can basically conclude that around a 35 at. % Fe we have a crossover in the magnetic behavior of our nanoparticles. Dipolar interactions, which were dominant at $x < 35$, are overcome by short-range ferromagnetic direct exchange interactions with increasing Fe content. Therefore, the ferromagnetic long-range order progressively prevails over the dipolar magnetic interactions and the nanoparticle anisotropy, and some kind of *magnetic percolation* takes place near 35 at. % Fe, like in other magnetically disordered systems of either metallic origin such as strongly correlated electron alloys of CeNiCu or oxide compounds with colossal magnetoresistance properties.[25–28]

B. ac magnetometry

In order to obtain more information about this crossover revealed by dc magnetic measurements it is relevant to study the dynamics of the superspins of our nanoparticles. Therefore ac susceptibility measurements have been carried out for three samples with different compositions: $x=24$, 35, and 39 (see Fig. 6). The applied magnetic field has been fixed at 0.3 mT and different frequencies have been used during the measurements, ranging from 0.03 to 1000 Hz. In all the range of temperatures analyzed ($5 < T < 300$ K), a frequency dependent maximum appears for every sample at a certain T_{max} for both the real (χ') and the imaginary (χ'') components of the magnetic susceptibility. Such maxima are associated to the freezing of the magnetic moments of the Fe nanoparticles with decreasing temperature. Moreover, above this T_{max} we have a dispersionless Curie-Weiss-type decrease in the $\chi'(T)$ curve while $\chi''(T)$ falls to zero with increasing temperature. All these phenomena clearly confirm the presence of a magnetic transition mediated by interactions at $T > T_{max}$, as previously indicated by the dc magnetic measurements. As the frequency of the applied magnetic field rises, the peak becomes smaller and shifts slightly to higher temperatures, as in many disordered systems such as canonical SG, reentrant SG, clustered oxides, etc.

We can determine again the Curie temperatures (T_C^*) by fitting $\chi'(T)$ to a Curie-Weiss expression or by the temperature at which χ'' becomes null. In both cases, the values of the Curie temperatures are close to those previously obtained by dc measurements within the experimental error ($<5\%$). The existence of the T_C^* corroborates that as the temperature rises and the thermal disorder increases, the influence of the interactions among the nanoparticles is reduced, and the system suffers a magnetic transition.

We have studied the dynamics of the magnetic moments at temperatures below T_C^*, by analyzing the evolution of the maximum appearing both in χ' and χ''. A systematic procedure has been followed. We have started by analyzing the shift of the peak position, δ, in χ' as a function of the frequency, $\omega = 2\pi f$, given by the expression
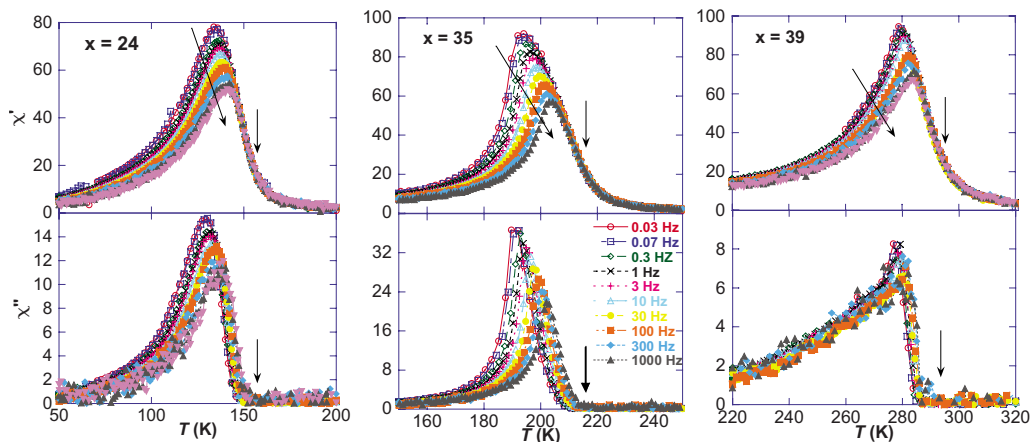

FIG. 6. (Color online) Real χ' and imaginary χ'' ac magnetic susceptibility components for Fe_xAg_{100-x} thin films ($x=24$, 35, and 39). The arrows indicate the evolution of the peak with increasing frequency (χ') and the position of the transition temperature.

TABLE III. δ, $z\nu$, and T_g parameters obtained from the fittings of χ' to a dynamical critical exponent activation law for Fe_xAg_{100-x} ($x=24$, 35, and 39).

	Freq. shift δ	Dynamical critical exponent law
$x=24$	0.010 ± 0.001	$z\nu=8.3 \pm 0.6$, $T_g=132.5 \pm 0.3$ K
$x=35$	0.009 ± 0.001	$z\nu=4.7 \pm 0.4$, $T_g=192.7 \pm 0.1$ K
$x=39$	0.0035 ± 0.0005	$z\nu=4.3 \pm 0.3$, $T_g=278.9 \pm 0.3$ K

$$\delta = \frac{\Delta T_{max}}{T_{max}\Delta(\log \omega)}, \tag{2}$$

where T_{max} corresponds to the peak temperature in the $\chi'(T)$ measurements. Depending on the magnetic behavior of the system, different values of δ have been found in the literature.[29] Therefore, we can compare the value of δ measured for our samples with those previously obtained in the literature, in order to get some idea about the dynamical magnetic behavior of our system during the freezing of the magnetic moments. As shown in Table III, the obtained values for δ are very small, close to those typically measured for spin glasses ($\delta=0.005$ Hz) but similar to $Fe_{20}Cu_{20}Ag_{60}$ nanopowders ($\delta=0.008$ Hz).[30] Because of the nanogranular nature of our Fe-Ag thin films, one would expect that the δ values would be more close to those typically obtained in cluster spin glass or SSG systems, which are an order of magnitude greater ($\delta \sim 0.05$–0.06 Hz).[29] This can be explained because the values of T_{max} measured in our samples are also much greater than those frequently obtained in the literature, and thereby, the value of $\delta(\propto 1/T_{max})$ is smaller than expected. Therefore, we can talk about a *glassy* state for our nanoparticles at low temperatures.

We have tried to get a deeper insight of the freezing process analyzing the variation of the peak temperature with the frequency. Since we have proven that magnetic interactions are important even in our most diluted samples, the typical Arrhenius relaxation for ideal SPM would lead to unrealistic results. Therefore we have used a phenomenological activation law and analyzed the magnetic behavior as is done in clustered magnetic systems and especially in SSG. It is necessary to probe the magnetic dynamics following a collective freezing. For this, we have tried a dynamical critical exponent activation law

$$\tau = \tau_0 \left(\frac{T_{max} - T_g}{T_g}\right)^{-z\nu} \tag{3}$$

being $z\nu$ precisely the critical exponent and T_g represents the freezing temperature of the magnetic moments of the nanoparticles when f approaches zero. Following standard procedures,[31] we have fixed τ_0 to 10^{-9} s, in order to be able to compare the results between the different samples studied. As can be seen in Fig. 7, a very good fitting has been obtained. An estimation of the error of the fittings is given by $\chi^2 = \Sigma[(\frac{y-y_i}{\sigma_i})^2]$ (the closer to 0 the better), where y is a fitted value for a given point, y_i is the measured data value and σ_i is an estimate of the standard deviation for y_i. In our case, we obtain that $\chi^2 = 0.0015$, 0.0079, and 0.0091 for the samples
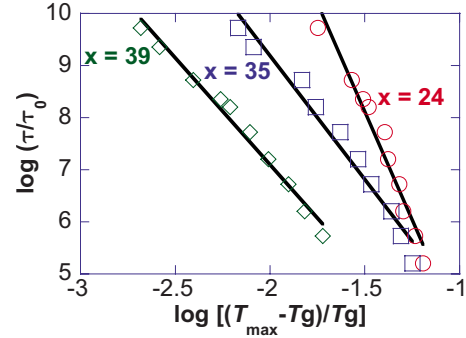

FIG. 7. (Color online) Logarithmic plots of τ/τ_0 vs $(T_{max}/T_g -1)$ for Fe_xAg_{100-x} thin films ($x=24$, 35, and 39) with their corresponding fits to a dynamical critical exponent activation law.

with $x=24$, 35, and 39. As shown in Table III, for $x=24$ the obtained value of $z\nu$ compares rather well with those reported on different spin glass systems ($5 < z\nu < 11$) as reviewed by Souletie and Tholence.[32] However there is a clear tendency for $z\nu$ to rapidly decrease with increasing Fe content, progressively approaching to those values corresponding to a mean-field phase transition ($z\nu \sim 2$). These results indicate that the interactions in our samples are strong enough so as to allow a cooperative behavior during the freezing of the magnetic moments.

A final test to analyze the nature of the collective freezing in our samples has been carried out by studying the so called Cole-Cole or Argand plots, χ'' vs χ'. A SPM system would exhibit an almost complete semicircle, as observed in magnetic molecule single crystals.[33] However, as depicted in Fig. 8, a strongly flattened semicircle is obtained for the sample with $x=24$, which is typical of a SSG system.[16] On the other hand, for the sample with $x=35$, for low frequencies (right-
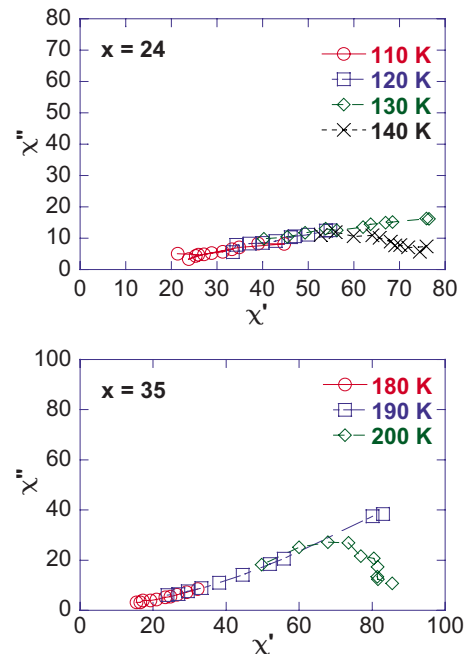

FIG. 8. (Color online) Cole-Cole plots, $\chi''(f)$ vs $\chi'(f)$, for two Fe_xAg_{100-x} samples with $x=24$ and 35.
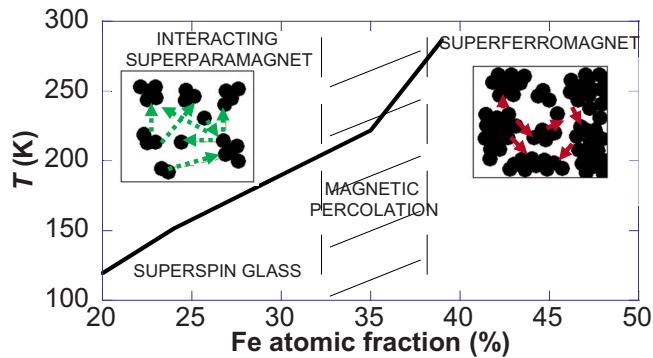
FIG. 9. (Color online) Magnetic phase diagram of Fe_xAg_{100-x} ($20 \leq x \leq 50$) granular thin films. In the insets a schematic representation of the arrangement of the nanoparticles and their main interactions (dipolar: dashed arrows/exchange: short continuous arrows) are depicted.

hand side) one finds a quarter circle, whereas at high frequencies (left-hand side) an increasing part with positive curvature appears. These features indicate a tendency of the system toward a SFM ordering[16] as the Fe concentration increases.

Therefore, the ac susceptibility analysis clearly indicates a crossover from a SSG to a SFM state near 35 at. %. Our results can be summarized by the magnetic phase diagram appearing in Fig. 9.

At low concentrations ($x < 35$), a magnetic transition mediated by interactions takes place at $T > T_C^*$, due to the increasing thermal disorder. This is revealed by the good fitting of the χ' decay to a Curie-Weiss transition and by χ'' becoming null at $T > T_C^*$. At these temperatures, the system behaves basically like an ISPM,[11] in which the individual nanoparticles and the clusters of the nanoparticles interact mainly by dipolar interactions. As the temperature decreases, during the freezing process, the system enters into a magnetically disordered state at low temperatures, as indicated by the obtained δ and $z\nu$ values. More specifically, the nanoparticles suffer a collective freezing with decreasing temperature into a SSG state, mediated mainly by dipolar interactions, the anisotropy of the nanoparticles and the spatial disorder in the arrangement of the nanoparticles.

With increasing Fe concentration a process of magnetic percolation takes place due to the more relevant role of direct exchange interactions with increasing Fe content. This enhances the long-range ferromagnetic order in our samples and makes the transitions displace toward higher temperatures. This is related to an increasing relevance of the direct exchange interactions among the nanoparticles. Finally, at x

> 35 the magnetic behavior is more similar to the one expected for a SFM. This implies that the nanostructured nature of our samples is already being lost because of the percolation and that regions of FM correlated particle moments appear with increasing Fe concentration. Therefore we can no longer only think in terms of a collective freezing of the nanoparticles. Specially illustrative is the clear change in the shape of χ'' for this sample in comparison to those with less Fe concentration (see Fig. 8). A similar SFM behavior was obtained by Bedanta *et al.* for CoFe nanoparticles embedded in an Al_2O_3 insulating matrix, although in our case we have associated it to the increasing importance of direct exchange interactions between the nanoparticles as their concentration increases and the system becomes magnetically percolated, rather than to the presence of small *glue nanoparticles* which allow a tunneling exchange between the bigger ones as proposed in Ref. 34.

Finally, it is necessary to remark that until now we have established as predominant in our samples the magnetic dipolar and direct exchange interactions, but other interactions, particularly, Ruderman-Kittel-Kasuya-Yosida interactions (RKKY) could also be playing a role. Nevertheless, in previous studies[35] theoretical calculations have been performed with the result that for nanoparticles with sizes above 1 nm, RKKY interactions are much less important than these two, specially at concentrations as high as those we are working with in our granular thin films.

IV. CONCLUSIONS

Fe_xAg_{100-x} ($20 \leq x \leq 50$) granular thin films composed of small Fe nanoparticles (2.5–3 nm) inside a Ag matrix have been prepared by sputtering deposition technique. The size of these nanoparticles remains nearly constant with increasing Fe content. Their magnetic characterization has revealed a definite crossover from a SSG to a SFM state around 35 at. %. This has been attributed to the magnetic percolation of the system motivated by the increasing importance of direct exchange interactions as the density of Fe nanoparticles increases.

---

[1] C. Binns, M. J. Maher, Q. A. Pankhurst, D. Kechrakos, and K. N. Trohidou, Phys. Rev. B **66**, 184413 (2002).

[2] J. Q. Wang and G. Xiao, Phys. Rev. B **49**, 3982 (1994).

[3] K. Sumiyama, Phys. Status Solidi A **126**, 291 (1991).

[4] A. García Prieto, M. L. Fdez-Gubieda, C. Meneghini, A. García-

Arribas, and S. Mobilio, Phys. Rev. B **67**, 224415 (2003).

[5] A. García Prieto, M. L. Fdez-Gubieda, J. Chaboy, M. A. Laguna-Marco, T. Muro, and T. Nakamura, Phys. Rev. B **72**, 212403 (2005).

[6] H. S. Nalwa, *Magnetic Nanostructures* (American Scientific,

California, 2002).

[7] M. L. Fdez-Gubieda, A. García Prieto, A. García Arribas, C. Meneghini, and S. Mobilio, Europhys. Lett. **59**, 855 (2002).

[8] L. Néel, Ann. Géophys. (C.N.R.S.) **5**, 99 (1949).

[9] G. Prinz, Science **282**, 1660 (1998).

[10] F. R. De Boer, R. Boom, W. C. M. Mattens, A. R. Miedema, and A. K. Niessen, *Cohesions in Metals* (North-Holland, Amsterdam, 1988), p. 233.

[11] P. Allia, M. Coisson, F. Spizzo, P. Tiberto, and F. Vinai, Phys. Rev. B **73**, 054409 (2006).

[12] J. Alonso, M. L. Fdez-Gubieda, L. Fernández Barquín, I. de Pedro, J. M. Barandiarán, I. Orue, A. Svalov, and G. Sarmiento, J. Appl. Phys. **105**, 07B513 (2009).

[13] P. Allia, M. Coisson, P. Tiberto, F. Vinai, M. Knobel, M. A. Novak, and W. C. Nunes, Phys. Rev. B **64**, 144420 (2001).

[14] W. Kleemann, O. Petracic, Ch. Binek, G. N. Kakazei, Y. G. Pogorelov, J. B. Sousa, S. Cardoso, and P. P. Freitas, Phys. Rev. B **63**, 134423 (2001).

[15] S. Sahoo, O. Petracic, Ch. Binek, W. Kleemann, J. B. Sousa, S. Cardoso, and P. P. Freitas, Phys. Rev. B **65**, 134406 (2002).

[16] O. Petracic, X. Chen, S. Bedanta, W. Kleemann, S. Sahoo, S. Cardoso, and P. P. Freitas, J. Magn. Magn. Mater. **300**, 192 (2006).

[17] S. Mørup, M. B. Madsen, J. Franck, J. Villadsen, and C. J. W. Koch, J. Magn. Magn. Mater. **40**, 163 (1983).

[18] M. El-Hilo, R. W. Chantrell, and K. O'Grady, J. Appl. Phys. **84**, 5114 (1998).

[19] M. Sasaki, P. E. Jonsson, H. Takayama, and H. Mamiya, Phys. Rev. B **71**, 104405 (2005).

[20] R. W. Chantrell, N. S. Walmsley, J. Gore, and M. Maylin, J. Appl. Phys. **85**, 4340 (1999).

[21] R. W. Chantrell, N. S. Walmsley, J. Gore, and M. Maylin, Phys.

[22] W. C. Nunes, L. M. Socolovsky, J. C. Denardin, F. Cebollada, A. L. Brandl, and M. Knobel, Phys. Rev. B **72**, 212413 (2005).

[23] L. Fernández Barquín, R. García Calderón, B. Farago, J. Rodríguez-Carvajal, A. Bleloch, D. McComb, R. Chater, and Q. A. Pankhurst, Phys. Rev. B **76**, 172404 (2007).

[24] A. García Prieto and M. L. Fdez-Gubieda, Physica B **354**, 92 (2004).

[25] N. Marcano, J. C. Gómez Sal, J. I. Espeso, J. M. De Teresa, P. A. Algarabel, C. Paulsen, and J. R. Iglesias, Phys. Rev. Lett. **98**, 166406 (2007).

[26] N. Marcano, J. C. Gómez Sal, J. I. Espeso, L. Fernández Barquín, and C. Paulsen, Phys. Rev. B **76**, 224419 (2007).

[27] E. Dagotto, *Nanoscale Phase Separation and Colossal Magnetoresistance: The Physics of Manganites and Related Compounds* (Springer-Verlag, Berlin, 2002).

[28] Y. Murakami, H. Kasai, J. J. Kim, S. Mamishin, D. Shindo, S. Mori, and A. Tonomura, Nat. Nanotechnol. **5**, 37 (2010).

[29] J. A. Mydosh, *Spin Glasses: An Experimental Introduction* (Taylor & Francis, London, 1993).

[30] D. H. Ucko, Q. A. Panckhurst, L. Fernández Barquín, J. Rodríguez Fernández, and S. F. J. Cox, Phys. Rev. B **64**, 104433 (2001).

[31] J. L. Tholence, Solid State Commun. **35**, 113 (1980).

[32] J. Souletie and J. L. Tholence, Phys. Rev. B **32**, 516 (1985).

[33] J. S. Miller and M. Drillon, *Magnetism: Molecules to Materials III* (Wiley-VCH, Weinheim, 2002), pp. 78–79.

[34] S. Bedanta, T. Eimüller, W. Kleemann, J. Rhensius, F. Stromberg, E. Amaladass, S. Cardoso, and P. P. Freitas, Phys. Rev. Lett. **98**, 176601 (2007).

[35] D. Altbir, J. d'Albuquerque e Castro, and P. Vargas, Phys. Rev. B **54**, R6823 (1996).

Rev. B **63**, 024410 (2000).